

# The effect of thickness in the through-diffusion experiment

## Final report

Matti Valkiainen, Hannu Aalto, Jarmo Lehikoinen &

Kari Uusheimo

VTT Chemical Technology



ISBN 951-38-4983-X  
ISSN 1235-0605  
Copyright © Valtion teknillinen tutkimuskeskus (VTT) 1996

JULKAISIJA – UTGIVARE – PUBLISHER

Valtion teknillinen tutkimuskeskus (VTT), Vuorimiehentie 5, PL 2000, 02044 VTT  
puh. vaihde (09) 4561, faksi (09) 456 4374

Statens tekniska forskningscentral (VTT), Bergsmansvägen 5, PB 2000, 02044 VTT  
tel. växel (09) 4561, fax (09) 456 4374

Technical Research Centre of Finland (VTT), Vuorimiehentie 5, P.O.Box 2000, FIN-02044 VTT, Finland  
phone internat. + 358 9 4561, fax + 358 9 456 4374

VTT Kemiantekniikka, Ympäristötekniikka, Otakaari 3 A, PL 1404, 02044 VTT  
puh. vaihde (09) 4561, faksi (09) 456 6390

VTT Kemiteknik, Miljöteknik, Otsvängen 3 A, PB 1404, 02044 VTT  
tel. växel (09) 4561, fax (09) 456 6390

VTT Chemical Technology, Environmental Technology, Otakaari 3 A, P.O.Box 1404,  
FIN-02044 VTT, Finland  
phone internat. + 358 9 4561, fax + 358 9 456 6390

Technical editing Leena Ukoski

VTT OFFSETPALVELU, ESPOO 1996

Valkiainen, Matti, Aalto, Hannu, Lehtikoinen, Jarmo & Uusheimo, Kari. The effect of thickness in the through-diffusion experiment. Final Report [Paksuuden vaikutus läpιδiffuusiokokeessa. Loppuraportti]. Espoo 1996, Technical Research Centre of Finland, VTT Tiedotteita - Meddelanden - Research Notes 1788. 30 p. + app. 3 p.

**UDC** 552:532.72:552.32

**Keywords** rocks, granite, rock mechanics, rock properties, diffusion, porosity, water, thickness, measurement, experimentation

## ABSTRACT

This report contains an experimental study of diffusion in the water-filled pores of rock samples. The samples studied are rapakivi granite from Loviisa, southern Finland. The drill-core sample was sectioned perpendicularly with a diamond saw and three cylindrical samples were obtained. The nominal thicknesses (heights of the cylinders) are 2, 4 and 6 cm. For the diffusion measurement the sample holders were pressed between two chambers. One of the chambers was filled with 0.0044 molar sodium chloride solution spiked with tracers. Another chamber was filled with inactive solution. Tritium (HTO) considered to be a water equivalent tracer and anionic  $^{36}\text{Cl}^-$  were used as tracers.

The through diffusion was monitored about 1000 days after which time the diffusion cells were emptied and the sample holders dismantled. The samples were sectioned into 1 cm slices and the tracers were leached from the slices. The porosities of the slices were determined by the weighing method.

The rock-capacity factors could be determined from the leaching results obtained. It was seen that the porosity values were in accordance with the rock capacity factors obtained with HTO. An anion exclusion can be seen comparing the results obtained with HTO and  $^{36}\text{Cl}^-$ . The concentration profile through even the thickest sample had reached a constant slope and the rate of diffusion was practically at a steady state. An anion exclusion effect was also seen in the effective diffusion coefficients.

The effect of thickness on diffusion shows that the connectivity of the pores decreases in the thickness range 2 - 4 cm studied. The decrease as reflected in the diffusion coefficient was not dramatic and it can be said that especially for studying chemical interactions during diffusion, the thickness of 2 cm is adequate.

Valkiainen, Matti, Aalto, Hannu, Lehikoinen, Jarmo & Uusheimo, Kari. The effect of thickness in the through-diffusion experiment. Final Report [Paksuuden vaikutus läpιδiffuusiokokeessa. Loppuraportti]. Espoo 1996, Technical Research Centre of Finland, VTT Tiedotteita - Meddelanden - Research Notes 1788. 30 p. + app. 3 p.

**UDC** 552:532.72:552.32

**Keywords** rocks, granite, rock mechanics, rock properties, diffusion, porosity, water, thickness, measurement, experimentation

## TIIVISTELMÄ

Tämä raportti perustuu Loviisan rapakivigraniitinäytteillä tehtyyn matriisidiffuusiotutkimukseen, jossa tutkittiin näytteen paksuuden vaikutusta diffuusion. Näytteet sahattiin timanttilaikalla kairansydäimestä akselia vastaan kohtisuoraan ja niiden paksuuksiksi valittiin 2, 4 ja 6 cm. Diffuusiokokeet tehtiin läpιδiffuusiogeometriassa, jossa näyte on sijoitettuna kahden nestetäyteen kammion väliin. Kammiot täytettiin 0,0044 molaarisella natriumkloridiliuoksella. Toiseen kammioista panostettiin merkkiainetta. Tritium (HTO), joka on vesiuskollinen merkkiaine, oli toisena komponenttina ja anioninen  $^{36}\text{Cl}$  toisena komponenttina.

Läpιδiffuusiota seurattiin noin 1 000 päivän ajan, jonka jälkeen diffuusiokammiot tyhjennettiin ja näytteenpitimet purettiin. Näytteet viipaloitiin 1 cm:n paksuisiksi ja viipaleista eluointiin merkkiaineet. Näytteiden huokoisuus määritettiin punnitusmenetelmällä.

Näytteiden kapasiteettitekijät voitiin määrittää eluutiotuloksista. Tritiumkapasiteettitekijät ja punnitushuokoisuustulokset olivat sangen yhtäpitäviä. Kun verrataan HTO ja  $^{36}\text{Cl}^-$  tuloksia, nähdään selvä anioniekskluusio, joka näkyy myös efektiivisissä diffuusiokertoimissa; osoittautui myös, että paksuinkin näyte oli saavuttanut vakiodiffuusionopeuden.

Diffuusiotuloksista voidaan päätellä, että tutkitulla rapakivigraniitilla huokosreittien liityntä toisiinsa vähenee alueella 2 - 4 cm. Vähenneminen ole suuruudeltaan dramaattista, ja voidaan päätellä, että varsinkin kemiallisten vuorovaikutusten tutkimisessa on ohuin, 2 cm:n näyte riittävän paksu.

## FOREWORD

This report forms the second part of a laboratory study of matrix diffusion in granite samples of different thicknesses. The previous part of the report is published in VTT Research Notes number 1556. The theoretical part (Chapter 2) is taken as such from the previous report, but the results are described concentrating on the new results after approximately one additional year of experimental time and the measures taken after the ending of the through-diffusion experiment.

The help of Kirsti Helosuo in the sampling of the diffusion test and that of Seppo Juurikkala in the sectioning of the samples is appreciated. The liquid scintillation analysis of the samples was continued by Hannu Aalto after the death of Kari Uusheimo in 1994.

# CONTENTS

ABSTRACT .....	3
TIIVISTELMÄ.....	4
FOREWORD .....	5
CONTENTS .....	6
1 INTRODUCTION.....	7
2 DIFFUSION IN POROUS MATERIAL.....	8
3 EXPERIMENTAL.....	12
3.1 Rock samples and diffusion measurements.....	12
3.1.1 Rock samples.....	12
3.1.2 Diffusion experiment.....	12
3.2 Sectioning and leaching of the samples.....	14
3.3 Porosity measurement.....	16
4 RESULTS 17	
4.1 Diffusion of the tracers .....	17
4.1.1 Approaching the steady state.....	19
4.2 Leaching of the sub-samples .....	20
4.3 Water-saturation porosities .....	23
4.4 Fitting of the diffusion model .....	23
5 DISCUSSION OF THE RESULTS.....	24
6 SUMMARY AND CONCLUSIONS.....	27
REFERENCES.....	29

## APPENDIX 1

### THE DERIVATIVES OF THE EXPERIMENTAL RESULTS

# 1 INTRODUCTION

Transport by diffusion from water-conducting fractures in a narrow pore network extending into the rock matrix is considered an important retardation mechanism in nuclear waste disposal. Radionuclides spread in the available pore space adjoining the fractures by diffusion.

In the laboratory the diffusion coefficients in the water phase are often determined from samples with rather short linear dimensions due to time limitations. In this study, the diffusion test is performed using three samples of rapakivi granite of different thicknesses. The samples were originally situated close to each other. The aim was to ensure the maximum possible homogeneity between the samples. The tracers used were tritium and  $^{36}\text{Cl}$ .

It has been reported in the literature /1, 2, 3/ that the geometrical formation factor measured for the rock samples decreases when the thickness of the sample increases. Because the geometrical formation factor  $F = \varepsilon^+ \sigma / \tau^2$ , where  $\varepsilon^+$  is the conducting porosity and  $\tau$  the length of the diffusion path divided by the thickness of the sample, tortuosity, it might be possible to see the effect of the sample thickness on the conductive porosity.

It was shown by Hemingway, Bradbury and Lever /4/ that the simple Fickian model does not provide a complete description of the concentration-time curves obtained for laboratory diffusion experiments. A new model was developed taking into account that some of the diffusion paths are dead-ends. The model characterizes dead-end pores with two parameters: the fraction of dead-end porosity from the total porosity and the average length of the dead-end pores.

The dead-end porosity model gives the same asymptotic behaviour and thus the same time-lag in through-diffusion geometry. A significant improvement for the interpretation of small-scale laboratory through-diffusion experiments was found. The fit of calculated diffusion behaviour to experimental data was found to better explain the pre-steady-state period of the through-diffused concentration.

Although the dead-end pore model better explains the laboratory-scale experiments, the conventional Fickian model was found to be adequate under all conditions likely to arise around the repository.

The tracers selected were tritium (HTO) and anionic  $^{36}\text{Cl}$ , easily analyzable by liquid scintillation counting. Both are considered as minimally sorbing.  $^{36}\text{Cl}$  is speciated as chloride, thus repulsive forces are expected between the ions and the pore walls. In the case of tritium, some interaction with the pore walls can be expected.

## 2 DIFFUSION IN POROUS MATERIAL

In the following model it is assumed that the concentration in the porewater is the same as in the surrounding water. The pores form a branching tortuous labyrinth, some branches are forming dead ends. Thus the porosity may be divided in two categories: through-transport and dead-end porosity. The rock-capacity factor is also divided in the same ratio in those two categories. The dead-end porosity concept has been applied to rock diffusion by Hemingway et al. at Harwell /4/ and later Lehtikoinen et al. /5/. The governing equation of their dead-end pore diffusion models is

$$\alpha^+ \frac{\partial C^+}{\partial t} + \alpha^* \frac{\partial C^*}{\partial t} = D_e \nabla^2 C^+ \quad (1a)$$

and

$$\frac{\partial C^*}{\partial t} = \frac{1}{t_t} (C^+ - C^*) \quad (1b)$$

where

- $C^+ = C^+(x,t)$  = concentration in the conductive pores,
- $C^* = C^*(x,t)$  = concentration in the dead-end pores,
- $D_e$  = effective diffusion coefficient<sup>1</sup>,
- $\alpha^+$  = rock-capacity factor of the conductive pores,
- $\alpha^*$  = rock-capacity factor of the dead-end pores,
- $t_t$  = relaxation time (characteristic time for diffusion into dead-end pores).

The partial differential equations (1a) and (1b) are solved in one dimension using the following trial function, which fulfils the initial condition  $\underline{C}(x,0)=0$  and boundary conditions  $\underline{C}(0,t)=C_1$  and  $\underline{C}(l,t)=0$ .

---

<sup>1</sup>The effective diffusion coefficient and the diffusion coefficient in an unconfined fluid are related through the so-called formation factor  $F$ :  $D_e = F \times D_w$ . The pore structure parameters and  $F$  can be interrelated. Skagius /4/ uses  $F = \varepsilon^+ \sigma / \tau^2$ , where  $\sigma$  is the constrictivity. The formation factor will thus be smaller than unity. Inverse notation is also used (e. g. Katsube et al. /5/).

$$\underline{C}(x,t) = C_1 \left( \frac{l-x}{l} \right) + \sum_{n=1}^{\infty} \sin \left( \frac{n\pi x}{l} \right) f_{\frac{C}{n}}(t) \quad (2)$$

where  $f_{\frac{C}{n}}(t)$  is some function of  $t$ ,  $l$  is the length of the specimen and  $\underline{C}$  has been selected to indicate that Eq.(3) is written for both  $C^+$  and  $C^*$ . By introducing (2) into (1) the solution looked for is found as

$$\frac{C^+(x,t)}{C_1} = \frac{l-x}{l} + \frac{2}{\pi} \sum_{n=1}^{\infty} \sum_{i=1}^2 \frac{1}{n} \sin \left( \frac{n\pi x}{l} \right) \frac{\beta_n^{(3-i)} (1 - t_i \beta_n^{(i)})}{\beta_n^{(i)} - \beta_n^{(3-i)}} e^{-\beta_n^i t} \quad (3a)$$

and

$$\frac{C^*(x,t)}{C_1} = \frac{l-x}{l} + \frac{2}{\pi} \sum_{n=1}^{\infty} \sum_{i=1}^2 \frac{1}{n} \sin \left( \frac{n\pi x}{l} \right) \frac{\beta_n^{(3-i)}}{\beta_n^{(i)} - \beta_n^{(3-i)}} e^{-\beta_n^i t} \quad (3b)$$

where  $\beta_n^{(i)}$  are the roots of the following second-order algebraic equation

$$\alpha^+ t_i \beta_n^2 - \left[ \alpha^+ + \alpha^* + t_i D_e \left( \frac{n\pi}{l} \right)^2 \right] \beta_n + D_e \left( \frac{n\pi}{l} \right)^2 = 0 \quad (4)$$

The results of the through-diffusion experiment can be expressed conveniently by the scaled ratio between the concentration in the measuring cell ( $C_2$ ) and the reservoir ( $C_1$ )

$$\begin{aligned} C_r(t) &= \frac{C_2 V_2}{C_1 A l} = \frac{Q(t)}{C_1 A l} = \\ &= \frac{D_e}{l^2} \left\{ t - 2 \sum_{n=1}^{\infty} \sum_{i=1}^2 (-1)^n \frac{\beta_n^{(3-i)} (1 - t_i \beta_n^{(i)})}{\beta_n^{(i)} (\beta_n^{(i)} - \beta_n^{(3-i)})} (1 - e^{-\beta_n^i t}) \right\} \end{aligned} \quad (5)$$

where  $A$ =cross-sectional area of rock plug in the diffusion experiment,  $V_2$ =the volume of the measuring cell and

where  $A$ =cross-sectional area of rock plug in the diffusion experiment,  $V_2$ =the volume of the measuring cell and

$$Q(t) = -AD_e \int_0^t \frac{\partial C^+(x, t')}{\partial x} \Big|_{x=l} dt' \quad (6)$$

corresponding to the diffused amount for the time  $t$ .

By scaling the time by the square of the thickness, the results of the samples of different thicknesses can be presented in the same  $t/l^2$ ,  $(C_2V_2)/(C_1A)$  -co-ordinates. As an example, we can take three rock samples, thicknesses 2, 4 and 6 cm.  $D_e = 2.3 \times 10^{-13}$  m<sup>2</sup>/s,  $\alpha = 0.004$ , dead-end-pore length  $l_{de} \approx (3tD_e/\alpha^+)^{1/2} = 2$  cm and  $\varepsilon^+ / (\alpha^+ + \varepsilon^*) = 0.5$ .

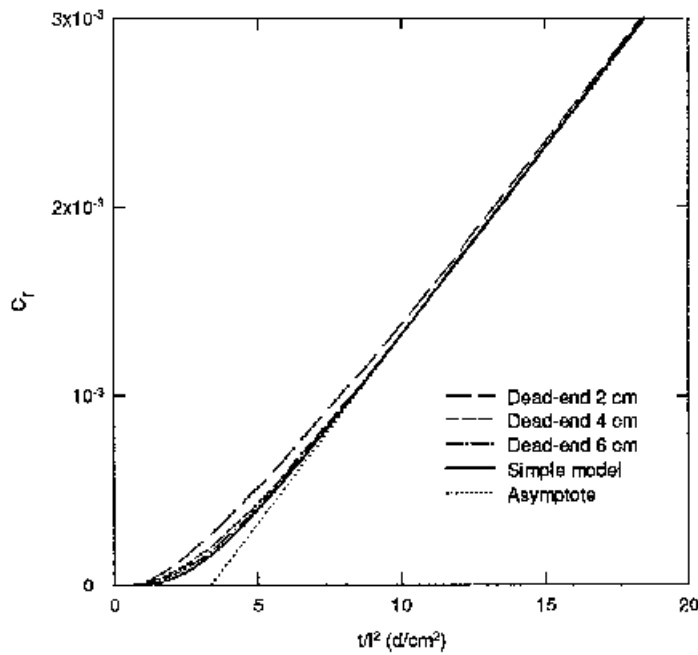


Figure 1. The initial period in diffusion experiment, calculated results for three examples, thicknesses 2, 4 and 6 cm.  $D_e = 2.3 \times 10^{-13}$  m<sup>2</sup>/s,  $\alpha = 0.004$ , length of the dead-end pores  $l_{de} = 2$  cm and  $\varepsilon^+ / (\alpha^+ + \varepsilon^*) = 0.5$ . The diffusion curves are scaled to the same scale and all have the same asymptote. The curve applying to all examples in the case without dead-end porosity is the lowest.

Figure 1 depicts the initial part of the calculated through diffusion. It can be seen that the effect of dead-end porosity is more pronounced in thinner samples. When the samples are thicker, the diffusion behaviour approaches the simple case, not taking into account dead-end porosity in calculations /6/

$$C_r(t) = \frac{D_e t}{l^2} - \frac{\alpha}{6} - \frac{2\alpha}{\pi^2} \sum_{n=1}^{\infty} \frac{(-1)^n}{n^2} \exp\left(\frac{D_e n^2 \pi^2 t}{l^2 \alpha}\right) \quad (7)$$

where  $\alpha = \alpha^+ + \alpha^*$ . The asymptotic behaviour of Eq.(7), as  $t \rightarrow \infty$ , is given by the line

$$C_r(t) = \frac{D_e t}{l^2} - \frac{\alpha}{6}$$

## 3 EXPERIMENTAL

### 3.1 ROCK SAMPLES AND DIFFUSION MEASUREMENTS

#### 3.1.1 Rock samples

During site selection studies for a repository for low and medium-level reactor waste, drill-holes were made at Hästholmen, Loviisa. Drill-core samples were obtained from Imatran Voima Oy originating from drill-hole Y1 between 195.15 m and 195.51 m. The rock is fine-grained rapakivi granite. The drill-core sample was sectioned perpendicularly with a fast, water-cooled diamond saw and three cylindrical samples were obtained. The nominal thicknesses (heights of the cylinders) were 2, 4 and 6 cm.

#### 3.1.2 Diffusion experiment

The rock samples were fixed with silicone glue to cylindrical openings in PVC frames of 2 mm larger diameter than the drill-cores, Figure 2.

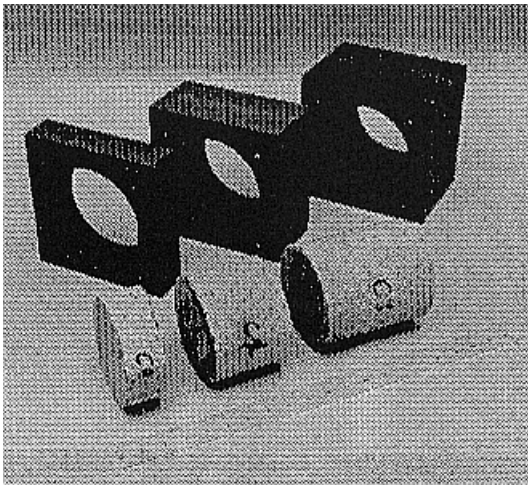


*Figure 2. Rock samples and sample holders made of PVC plastic.*

After gluing, the rock samples were kept in the vacuum for 2 - 4 days to expel the air from the pore space. While in the vacuum, sodium chloride solution

(0.0044 molar) was put into contact with the samples. They were allowed to equilibrate with the solution for 1 - 10 months. For the diffusion measurement, the sample holders were pressed between two chambers 64 ml each in volume (Figure 3). One of the chambers was filled with 0.0044 molar sodium chloride solution spiked with tracers. Another chamber was filled with inactive solution. Tritium (HTO) considered to be a water-equivalent tracer and anionic  $^{36}\text{Cl}$  were used as tracers. The initial activity concentrations were with 2 cm and 4 cm samples about 2  $\mu\text{Ci/ml}$  about 1  $\mu\text{Ci/ml}$  for tritium and  $^{36}\text{Cl}$ , respectively. More activity was used with the thickest sample, about 8  $\mu\text{Ci/ml}$  HTO and 4  $\mu\text{Ci/ml}$  chloride-36.

activity was used with the thickest samples about 8  $\mu\text{Ci/ml}$  HTO and 4  $\mu\text{Ci/ml}$  chloride-36.

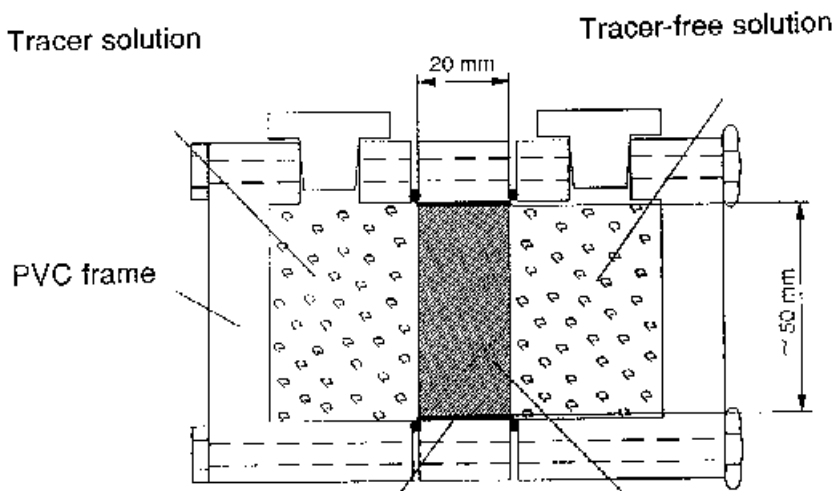


Figure 3. The experimental setup for the diffusion measurement, the rock sample separates the two liquid-filled chambers.

Table 1 shows a summary of the characteristics of the samples and equilibration times.

Table 1. Summary of the characteristics of the samples and equilibration times.

Sample	Length (mm)	Weight (g)	Diameter (mm)	Equilibration time (Months)
C1	19.3	104.66	51.6	1
C2	39.3	213.63	51.6	4
C3	58.8	320.65	51.6	10

The experiment was followed by taking samples from the originally inactive chamber. The water in the chamber had turned slightly radioactive. To begin the samples were taken originally weekly, later monthly. The chamber was emptied fully and filled again with new inactive solution. A sample of 10 ml was taken from the used solution for determination of the  $^3\text{H}$  and  $^{36}\text{Cl}$  content of the solution with a liquid scintillation counter.

### 3.2 SECTIONING AND LEACHING OF THE SAMPLES

The diffusion experiment was monitored over 1000 days, after which it was considered to have given all the essential information obtainable from the performed test phase. The measurement was interrupted by emptying and flushing the chambers. The rock specimens were removed from the PVC frames and sliced perpendicularly to the axis with a slow-speed diamond saw. Figure 4 presents the sample codes given to identify the sectioned samples. During sawing the samples lost some water and tracers. To minimize this, aluminium foil was used to wrap the samples to the extent possible.

The samples were leached individually at 100 ml of 0.044 Mol NaCl solution, initially free of radioactive tracers. The leachant was sampled regularly for activity determination and the sample was replaced with fresh solution. The leaching was monitored for 170 days.

Strong  
solution

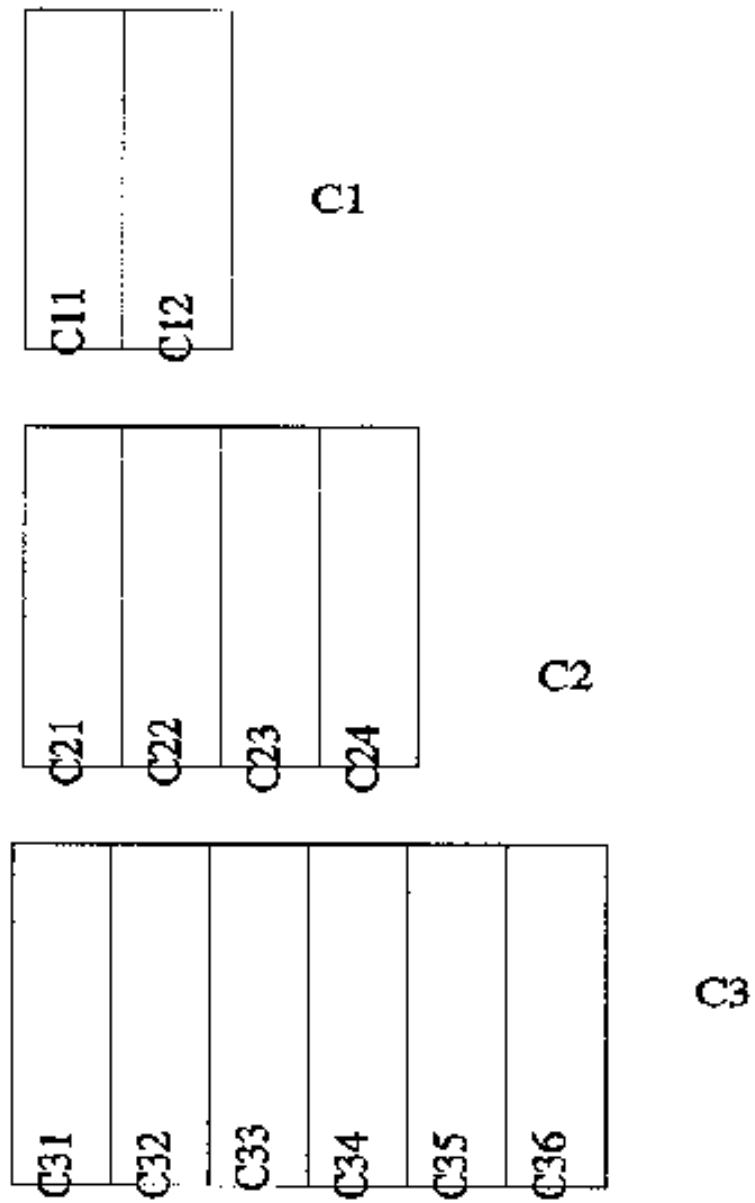


Figure 4. Sectioning and coding of the rock samples after the through-diffusion experiment.

### 3.3 POROSITY MEASUREMENT

The porosity of the sectioned sub-samples was measured after the leaching by a modified method of the Melnyk & Skeet-method [7]. The essential part of the method is the determination of the surface-dry, otherwise water-saturated weight of the sample by monitoring of the initial part of the drying process.

The rock slices were assumed to be completely water saturated after the leaching. They were weighed in water (one at a time), the extra moisture on the surface was slightly wiped off before placing in a balance, where the weight-loss during evaporation was monitored. Figure 5 shows the weight as a function of time for one of the sub-samples and determination of the surface-dry weight as the crossing point of two asymptotes.

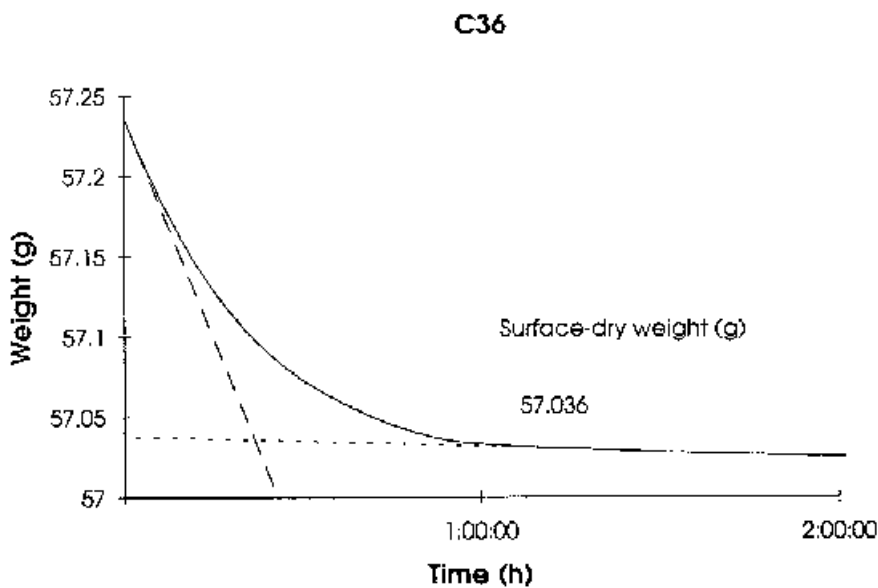


Figure 5. Determination of surface-dry weight as the crossing point of two asymptotes of the drying curve [7].

## 4 RESULTS

### 4.1 DIFFUSION OF THE TRACERS

Figures 6 and 7 show the cumulative amount of tracer diffused through the specimens as a function of time. The results are scaled to the same initial activity. There are disturbances in the final part of the experiment with the 2 cm sample, and therefore the 5 last data points were rejected.

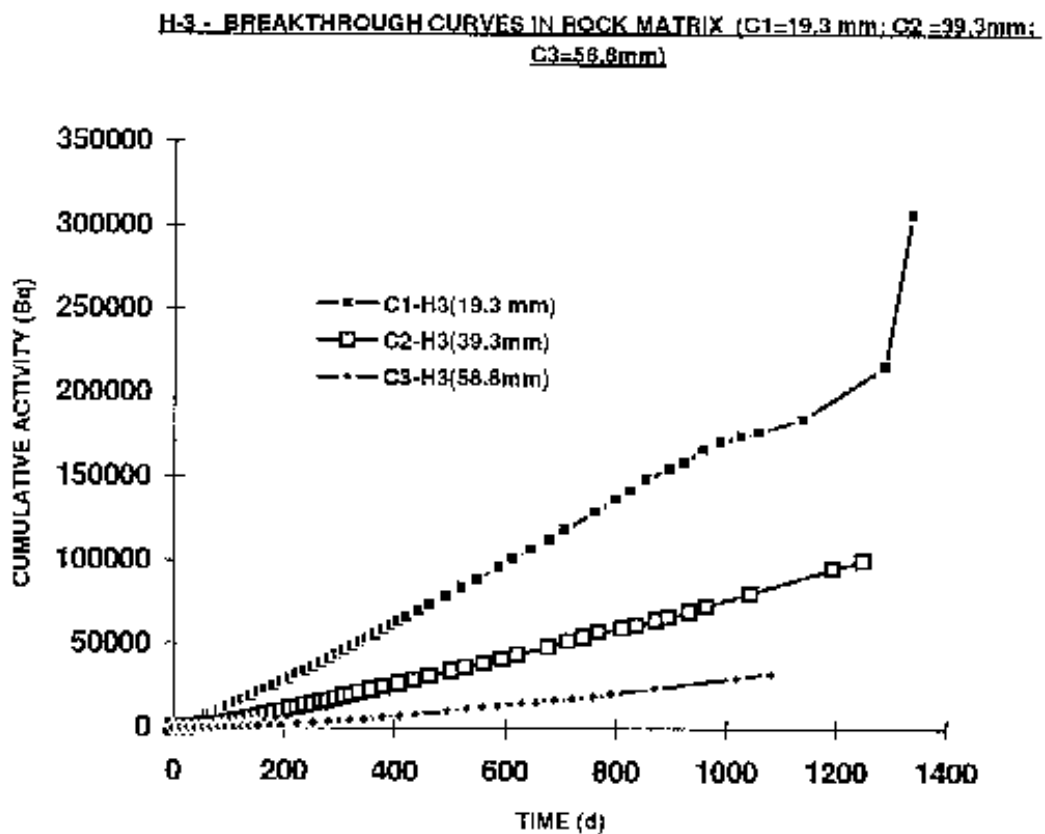


Figure 6. The amount of tritium diffused through rock samples of different thicknesses.

To simplify the presentation of the fitting of the experimental results, the data were transformed to the same co-ordinates used in Figure 1; the co-ordinates reveal the relative evolution of the three parallel experiments. See Figures 7 and 8, where only the initial part of the results of sample C1 are shown.

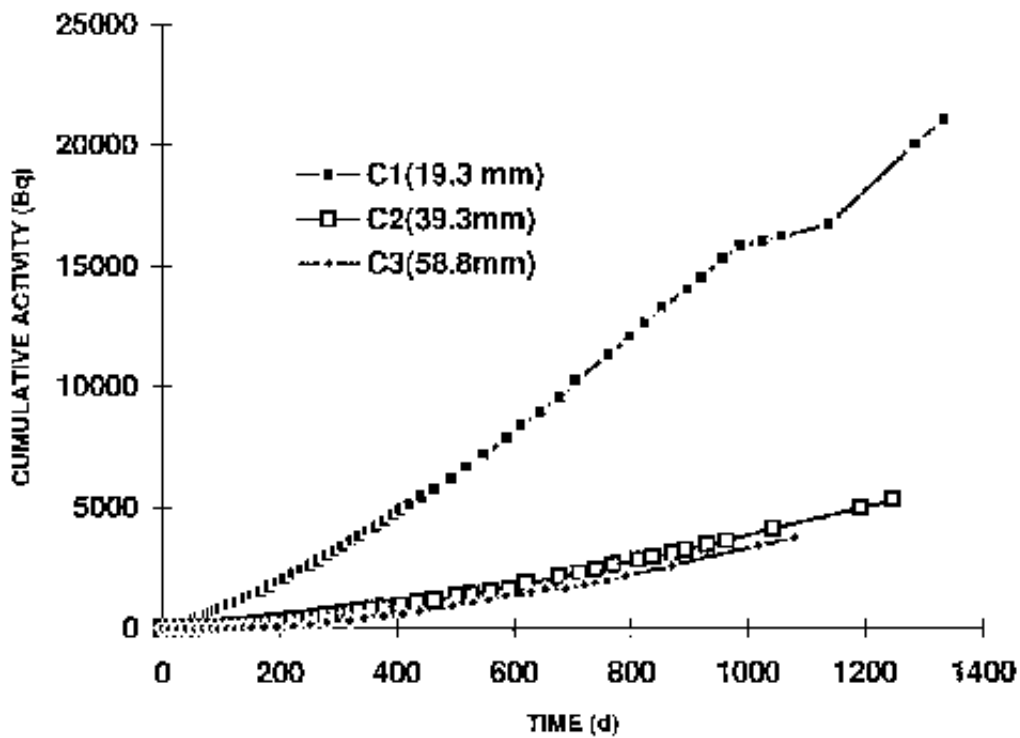


Figure 7. The amount of  $^{36}\text{Cl}$  diffused through rock samples of different thicknesses.

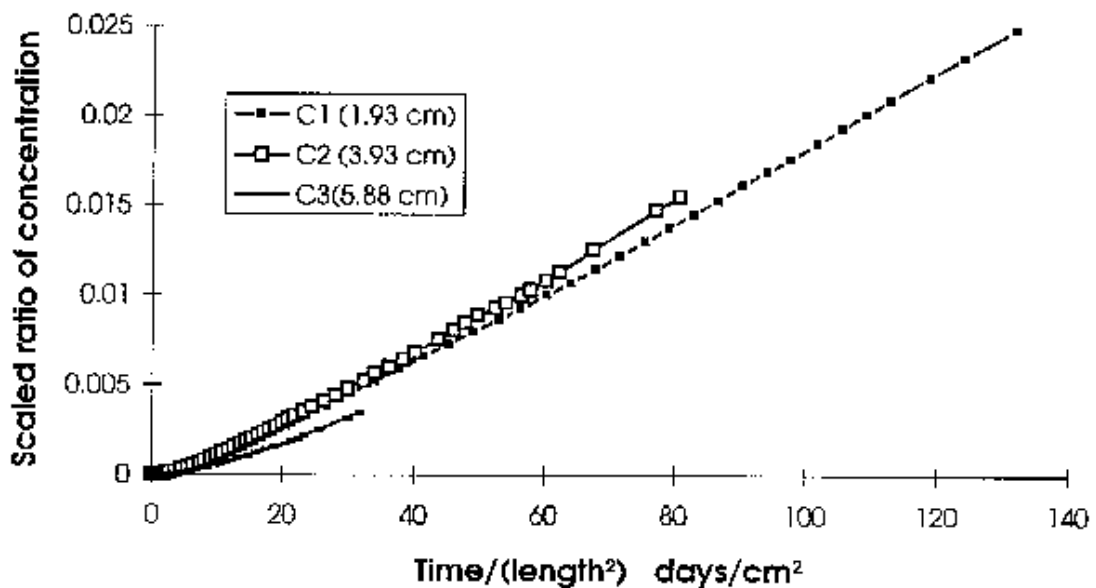


Figure 8. The experimental curves showing diffusion of HTO. The diffusion curves are scaled to the same scale and all would have the same asymptote in the ideal case, see figure 1. Only the initial part of the results of sample C1 are shown.

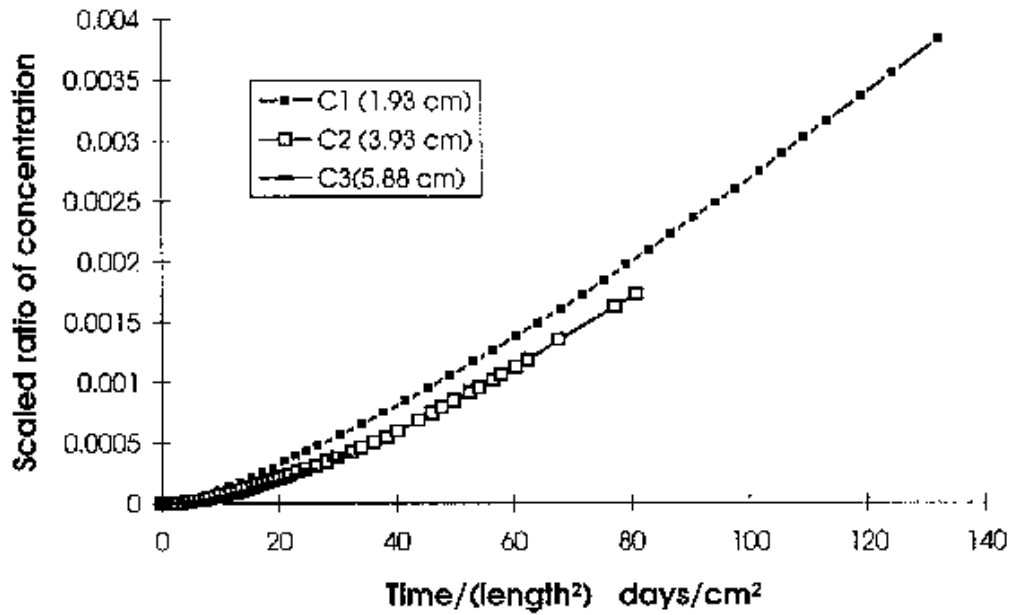


Figure 9. The experimental curves showing diffusion of  $^{36}\text{Cl}$ . The diffusion curves are scaled to the same scale and all would have the same asymptote in the ideal case, see Figure 1. Only the initial part of the results of sample C1 are shown.

#### 4.1.1 Approaching the steady state

The rate of the through-diffusion should stabilize to a constant value furnishing the effective diffusion coefficient. The through-diffused incremental amounts are presented as a function of time in Appendix 1. It can be said that the quality of the data does not permit exact estimation of the steady state of the through-diffusion, but the following can be stated.

- In the 2 cm sample the diffusion seems to obtain a stationary rate around 200 days, but after that the rate rises again. This behaviour is not seen with  $^{36}\text{Cl}$ .
- The 4 cm sample has achieved the steady-state phase.
- The 6 cm sample is at the beginning of the steady-state phase.

Visually estimated stationary levels gave the values for  $D_e$  given in Table 2.

Table 2. Effective diffusion coefficients estimated from the incremental amounts of the through-diffusion.

Tracer	Effective diffusion coefficients (m <sup>2</sup> /s)		
	C1 (2 cm)	C2 (4 cm)	C3 (6 cm)
<sup>3</sup> H	2.4 x 10 <sup>-13</sup>	2.2 x 10 <sup>-13</sup>	1.7 x 10 <sup>-13</sup>
<sup>36</sup> Cl	5.4 x 10 <sup>-14</sup>	3.5 x 10 <sup>-14</sup>	2.2 x 10 <sup>-14</sup>

#### 4.2 LEACHING OF THE SUB-SAMPLES

The tracer distribution inside the sample at the end of the diffusion experiment is approximately obtained from the leaching results of the sub-samples. Figure 10 shows an example of diffusion of <sup>3</sup>H and <sup>36</sup>Cl from a sub-sample.

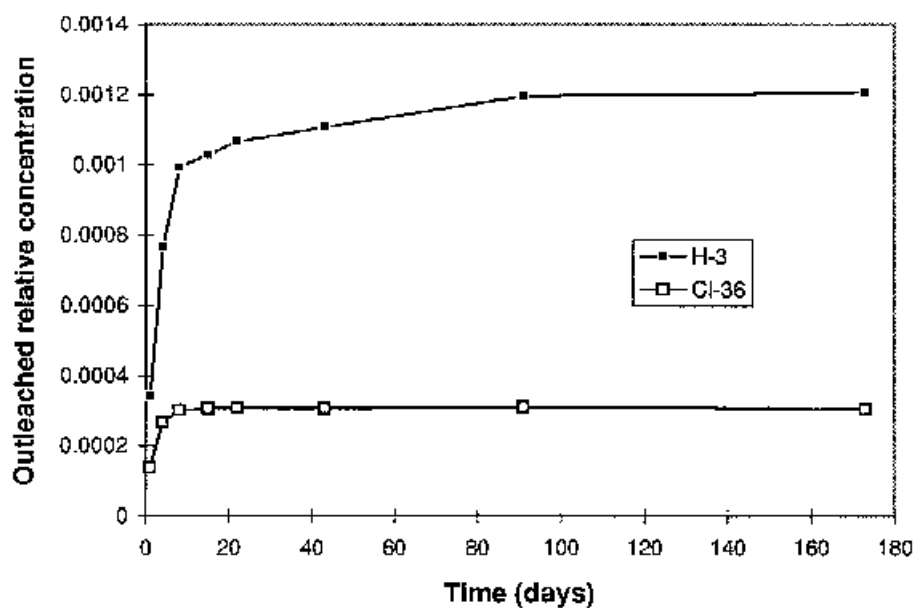


Figure 10. Leaching of tritium and <sup>36</sup>Cl from the sub-sample C23.

The rock-capacity factors were calculated as  $2 * \Sigma(Q_{\text{rock}}/V_{\text{rock}})/C_{\text{liquid}}$ , where  $Q_{\text{rock}}/V_{\text{rock}}$  is the outleached concentration of the individual rock slices and  $C_{\text{liquid}}$  is the concentration of tracer in the reservoir of high concentration. The factor 2 comes from two assumptions: 1) there has been zero concentration in the reservoir of high concentration and 2) the concentration gradient was linear, that is that the diffusion process had reached the steady state. The values for  $\alpha$ , which are shown in Figures 11 - 13, range for  $^3\text{H}$  from 0.0024 to 0.003 and for  $^{36}\text{Cl}$  from 0.0008 to 0.001.

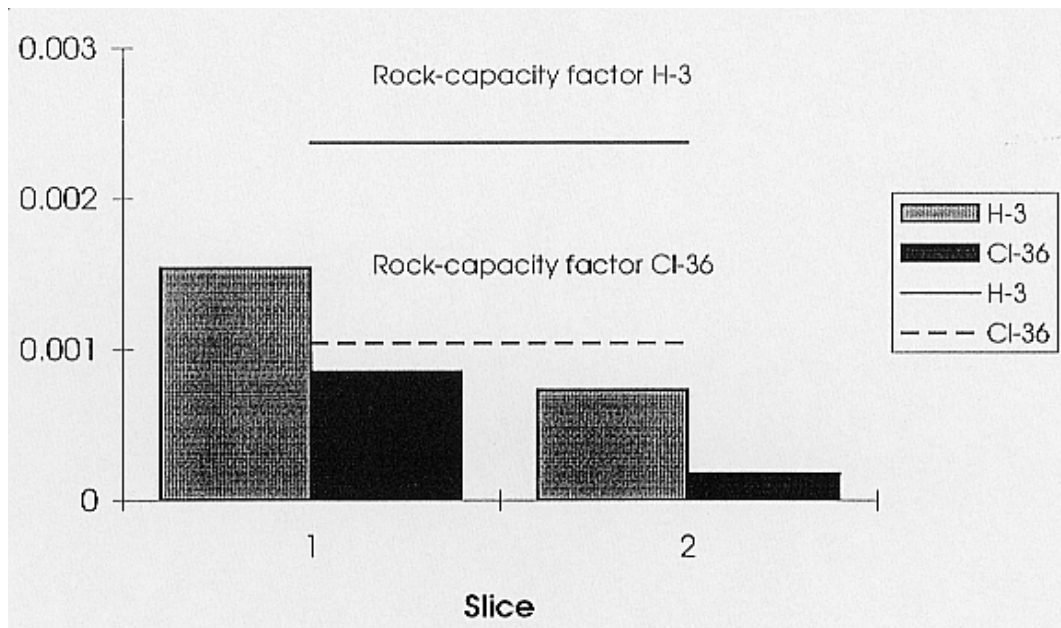


Figure 11. The average concentration of tracers in 1 cm-thick sub-samples of initially 2 cm-thick sample after 1335 days. The corresponding rock-capacity factors are calculated.

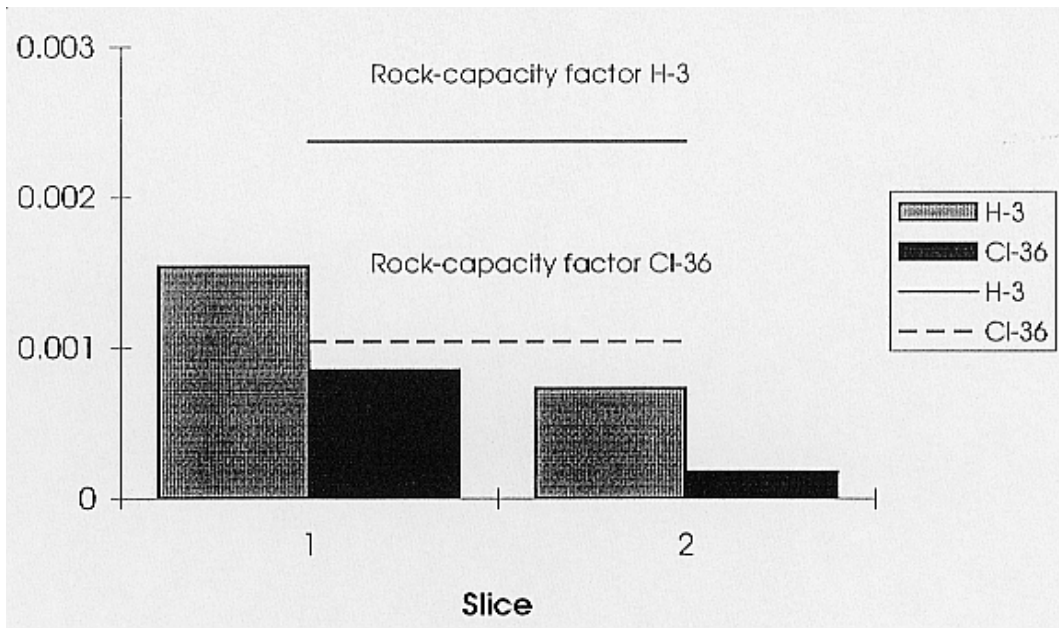


Figure 12. The average concentration of tracers in 1-cm thick sub-samples of initially 4-cm thick sample after 1248 days. The corresponding rock-capacity factors are calculated.

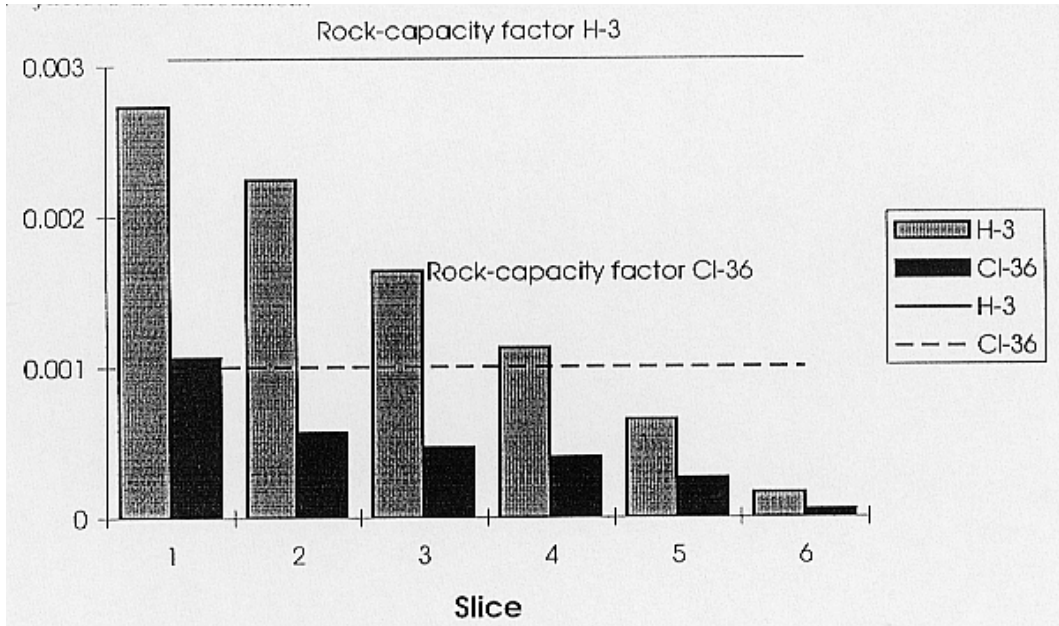


Figure 13. The average concentration of tracers in 1-cm-thick sub-samples of initially 6-cm thick sample after 1080 days. The corresponding rock-capacity factors are calculated.

### 4.3 WATER-SATURATION POROSITIES

The porosity values in Table 3 are obtained from the weight difference of the saturated, surface-dry sample and the same sample, dried at elevated temperature. The drying was carried out for four weeks at 40 °C and subsequently for two weeks at 60 °C.

*Table 3. Porosities of the sub-samples evaluated from the weight loss during drying.*

Sample code	Weight in water (g)	Weight (g) Surface dry	Weight (g) Dried 105 d	Density Saturated (g/cm <sup>3</sup> )	Porosity
C11	30.47	48.96087	48.9042	2.65	0.31%
C12	33.2	53.42751	53.3604	2.64	0.33%
C21	32.44	52.2087	52.1263	2.64	0.42%
C22	27.41	43.93125	43.8813	2.66	0.30%
C23	29.37	47.27531	47.2260	2.64	0.28%
C24	38.76	62.43638	62.3722	2.64	0.27%
C31	34.27	55.10786	55.0467	2.64	0.29%
C32	31.87	51.18599	51.1251	2.65	0.32%
C33	28.87	46.45416	46.3985	2.64	0.32%
C34	30.3	48.74763	48.6850	2.64	0.34%
C35	31.03	49.94936	49.8815	2.64	0.36%
C36	35.42	57.03562	56.9464	2.64	0.41%

### 4.4 FITTING OF THE DIFFUSION MODEL

In the previous report /8/, the numeric computation software MATLAB and Equation (5) were used to perform the fittings. Simplex-algorithm was used to minimize the sum of squares of the difference between the measured and calculated values. Fitting was performed by allowing all the 4 parameters to be adjusted to find the best fit. The fitted diffusion curves were shown in the previous report /8/.

## 5 DISCUSSION OF THE RESULTS

The effective diffusion coefficient  $D_e$  and the rock-capacity factor  $\alpha$  are obtained from the time-lag curve by fitting an asymptote in the steady-state part of the diffusion curve. One then presumes that the stationary behaviour is obtained. It was seen in the example in Figure 1 that the effect of the dead-end parameters decreases when the thickness of the sample increases. Figure 14 shows the calculated deviation from the asymptotic behaviour as a function of time divided by the square of the sample thickness for the 2 cm sample. The parameters for the dead-end model are the same as in Figure 1. For clarity purposes, the corresponding curves for 4 cm and 6 cm samples are not drawn; they would lie in the vicinity of the curve presenting the simple model. It can be seen that in the case of the diffusion behaving according to the simple model, asymptote describes well the through-diffusion after  $\text{time}/(\text{length})^2 \geq 10 \text{ days}/\text{cm}^2$  and according to the dead-end model (in the case of the example) after  $\text{time}/(\text{length})^2 \geq 20 \text{ days}/\text{cm}^2$ .

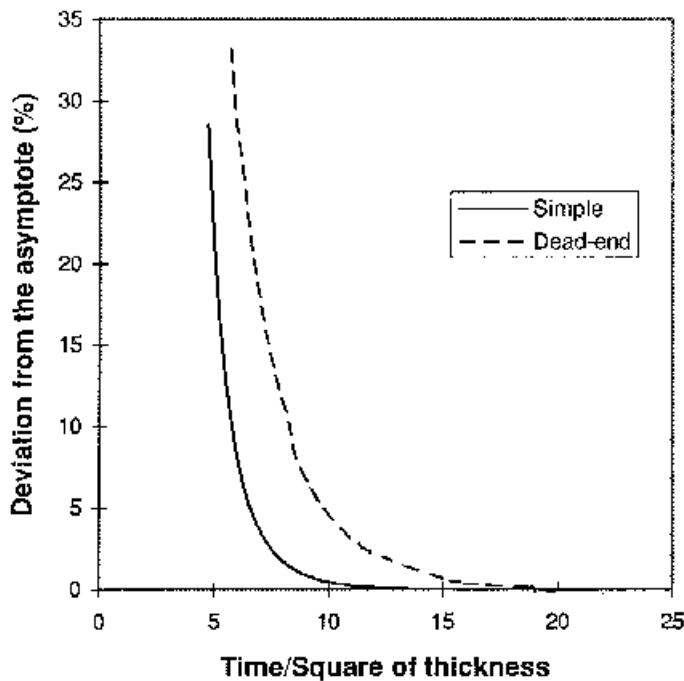


Figure 14. The calculated deviation from the asymptotic behaviour as a function of time divided by the square of the sample thickness for the 2 cm sample. The parameters for the dead-end model are same as in Figure 1. The unit for the x-axe is  $\text{days}/\text{cm}^2$ .

Asymptotes were fitted to the through-diffusion data presented (Figures 6 and 7). The effective diffusion coefficient  $D_e$  and the rock-capacity factor  $\alpha$  were obtained from the slope and the interception of the asymptote with x-axis, respectively. Table 4 shows the data obtained.

Table 4. Parameters obtained with the time-lag method fitting the asymptote to different parts of the slope of through-diffusion data.

$t_1$ (d)	$t_2$ (d)	$(t/l^2)_1$ (d/cm <sup>2</sup> )	$(t/l^2)_2$ (d/cm <sup>2</sup> )	$D_e$ ( <sup>3</sup> H) (m <sup>2</sup> /s)	$\alpha$ ( <sup>3</sup> H) (%)	$D_e$ ( <sup>36</sup> Cl) (m <sup>2</sup> /s)	$\alpha$ ( <sup>36</sup> Cl) (%)
2 cm							
169	253	45.4	67.9	$2 * 10^{-13}$	0.68	$3.4 * 10^{-14}$	0.24
267	337	71.7	90.5	$2.1 * 10^{-13}$	1.53	$3.9 * 10^{-14}$	0.42
351	587	94.2	157.6	$2.4 * 10^{-13}$	1.80	$4.4 * 10^{-14}$	0.66
4 cm							
266	502	17.2	32.5	$2.2 * 10^{-13}$	0.54	$2 * 10^{-14}$	0.80
713	1248	46.2	80.8	$2.5 * 10^{-13}$	1.3	$3.3 * 10^{-14}$	0.35
6 cm							
720	1080	20.8	31.2	$1.7 * 10^{-13}$	0.7	$2.3 * 10^{-14}$	0.13

When the asymptote is drawn using the data of the latter phase and  $\alpha$  is estimated from the time-lag, it is found to exceed the porosity and outleaching values in the case of <sup>3</sup>H and the outleaching in the case of <sup>36</sup>Cl. In the case of tritium, a value of  $\alpha$  near the water-saturation porosity obtained by the weighing method is expected. Taking the geometrical porosity to be 0.003 and applying formula  $\alpha = \epsilon + K_d \rho$ , a value of 0.018 for  $\alpha$  would give  $K_d = 5.7 * 10^{-6} \text{ m}^3/\text{kg}$ , and  $\alpha = 0.007$  would give  $K_d = 1.5 * 10^{-6} \text{ m}^3/\text{kg}$ . These values are in accordance with those obtained for granite from Kivetty by Puukko et al. /9/.

It is also seen that the linear asymptotic behaviour does not take place as predicted by both the simple Fickian and the dead-end model. The observed acceleration of the through diffusion may be caused by either some failure in the experimental setup or the pore system of the sample. Assuming that the results reflect the behaviour of the sample, there might be two explanations: the rock slowly weathers during the test making the pore system more open /10/. The other possible explanation is the assumption that in the rock there are different sets of diffusion paths with differing diffusivities. Thus the through-diffusion curve would be the sum of those penetration processes.

The concept of markedly different diffusion paths through the specimen would imply the specimens to be too small to be representative. However, autoradiographically visualized pores in rapakivi granite, which were impregnated with labelled PMMA, show microfissures, which are more than 10 mm long /11/. It has been estimated that in the case of a cubic grid, the necessary amount of cells is about  $15 * 15 * 15$  for the characterization of the transport properties of the material /12/. The rapakivi studied has a grain-size about 2 mm. Using the mentioned grid size as a rule of thumb, linear dimensions for the representative sample would lie between 30 and 150 mm. Comparing the results in Figures 6 and 7 it can be said that the 2 cm sample represents well enough the rock, especially in the cases where the chemical interactions of tracers and pore walls are studied.

The use of the dead-end porosity model for fitting was reported and discussed in the previous report /8/. It was intended to be continued in this final report, but due to the unsteady long-term behaviour of the sample, it is not favourable to have two additional fitting parameters.

## 6 SUMMARY AND CONCLUSIONS

The research summarized above was initialized as a study of the effect of thickness in through-diffusion of rapakivi granite samples. The fluid used to saturate the pores was 0.0044 molar NaCl and tracers used were HTO and  $^{36}\text{Cl}$ . The thicknesses of the samples were 2 cm, 4 cm and 6 cm. Because the progress of the diffusion through a sample is proportional to the square of the sample thickness, the necessary follow-up times are related as 1:4:9, respectively.

The through-diffusion was monitored for about 1000 days after which time the diffusion cells were emptied and the sample holders dismantled. The samples were sectioned to 1 cm slices and the tracers were leached from the slices. The porosities of the slices were determined by the weighing method.

The rock-capacity factors could be determined from the leaching results obtained. It was seen that the porosity values are in accordance with the rock-capacity factors obtained with HTO. An anion exclusion can be seen comparing the results obtained with HTO and  $^{36}\text{Cl}$ . The concentration profile through even the thickest sample had reached a constant slope and the rate of diffusion was practically at a steady state. The diffusion rates obtained from the slopes show a decreasing tendency as a function of thickness, indicating that the conductive porosity decreases as a function of the thickness. An anion exclusion effect is also seen in the effective diffusion coefficients.

Both the simple diffusion model and a model taking into account the effect of dead-end pores were applied in the interpretation of the through-diffusion curves. The crossing of the asymptote of the diffusion curves with the x-axis gives in both cases the rock-capacity factor, provided that the model describes well the experiment. It was observed that the tendency of the slopes of the through-diffusion curves was to increase also after a "pseudo steady state" had been reached for the through diffusion. The phenomena behind this effect is probably also responsible for the fact that the values of the rock-capacity factors obtained both from the time-lag method and the curve fitting are larger than from the leaching data. The results indicate that there is a parallel slow route in addition to the main diffusion pathway. This is either in the rock itself or it is a material property of the silicone seal surrounding the cylindrical sample.

The dead-end porosity model gives the same effective diffusion coefficient and rock-capacity value as the time-lag method; the deviation from the simple diffusion model is seen in the initial part of the through-diffusion curve causing a slower approach to the asymptotic behaviour.

The effect of thickness on diffusion shows that the connectivity of the pores

decreases in the thickness range 2 - 4 cm studied. The decrease as reflected in the diffusion coefficient was not dramatic and it can be said that especially for studying chemical interactions during diffusion, the thickness of 2 cm is adequate.

## REFERENCES

1. Bradbury M. H. and Green A., Retardation of Radionuclide Transport by Fracture Flow in Granite and Argillaceous Rocks. AERE-G 3528. Harwell: UKAEA, 1985. 16 p.
2. Skagius K. and Neretnieks I., Diffusion in crystalline rocks of some sorbing and nonsorbing species. Stockholm: KBS, 1982 Technical Report 82-12. 21 p. + 20 p. app.
3. Kumpulainen H. and Uusheimo K., Diffusivity and electrical resistivity measurements in rock matrix around fractures. Helsinki: Nuclear Waste Commission of Finnish Power Companies, 1989. Report YJT-89-19. 40 p. + 5 p. app.
4. Hemingway, S. J., Bradbury, M. H. and Lever, D.A. The effect of dead-end porosity on rock-matrix diffusion. Harwell, AERE. Theoretical Physics and Technology Divisions, 1983. Report AERE-R-10691. 43 p. + 9 figs.
5. Lehtikoinen, J., Muurinen, A., Olin, M., Uusheimo, K. and Valkiainen, M. Diffusivity and porosity studies in rock matrix. The effect of salinity. Espoo: Technical Research Centre of Finland, 1992. VTT Research Notes 1394. 28 p.
6. Crank, J. The mathematics of diffusion. 1st ed. Oxford, Clarendon Press, 1957. 347 p.
7. Melnyk, T. W. and Skeet M. M., An improved technique for the determination of rock porosity, Can. J. Earth Sci. 1986. Vol. 23, pp. 1068 - 1074.
8. Lehtikoinen, J., Uusheimo, K. and Valkiainen, M. The effect of thickness in the through-diffusion experiment. Espoo Technical Research Centre of Finland, 1994. VTT Research Notes 1556. 22 p. + app. 11 p.
9. Puukko, E., Heikkinen, T., Hakanen, M. and Lindberg, A., Diffusion of water, cesium and neptunium in pores of rocks. Helsinki: Nuclear Waste Commission of Finnish Power Companies, 1993. Report YJT-93-23. 31 p. + 27 p. app.
10. Uusheimo K. and Muurinen A., Effect of sodium chloride concentration on diffusivity in rock matrix. Helsinki: Nuclear Waste Commission of Finnish Power Companies, 1990. Report YJT-90-11. 15 p. + 4 p. app.

11. Hellmuth K. H. and Siitari-Kauppi M., Investigation of the porosity of rocks. Impregnation with  $^{14}\text{C}$ -polymethylmethacrylate (PMMA), a new technique. Helsinki: Finnish Centre for Radiation and Nuclear Safety, 1990. Report STUK-B-VALO 63. 67 p.
12. Dullien, F. A. L., Characterization of porous media - Pore level. Transport in porous media, 1991. Vol. 6, pp. 581 - 606.

## THE DERIVATIVES OF THE EXPERIMENTAL RESULTS

In the following are the graphical presentations of the through-diffused incremental amounts of the tracer divided by the time increment presented as a function of time together with a line drawn through the last data points. The corresponding diffusion coefficient is seen in each figure.

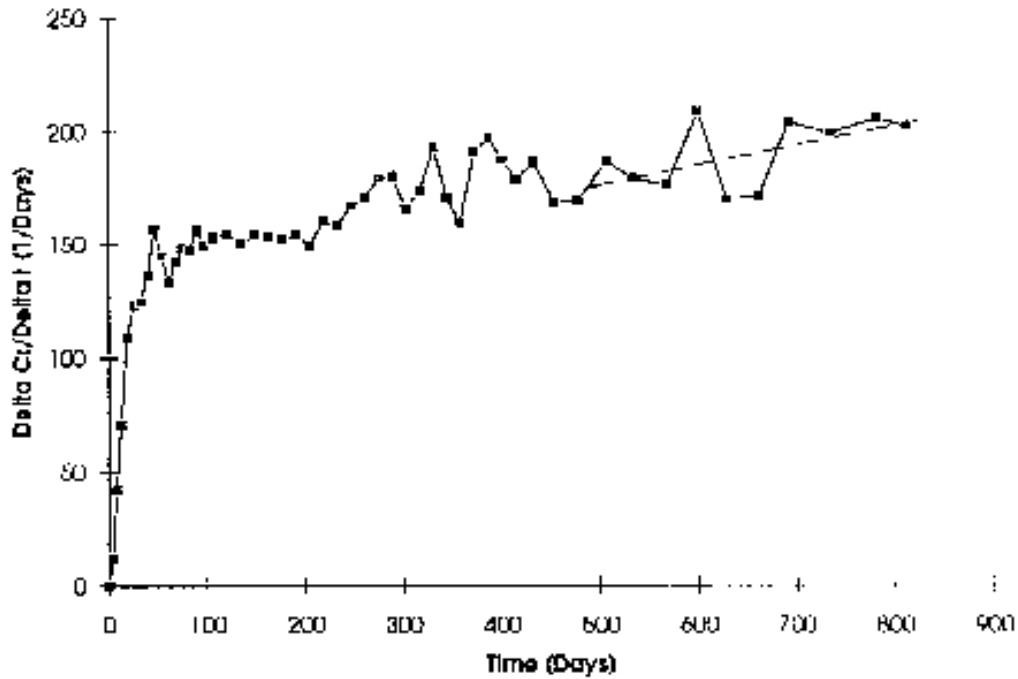


Figure 1 a) Sample C1, 2 cm. The incremental through-diffused amount divided by the time increment,  $^3\text{H}$ .

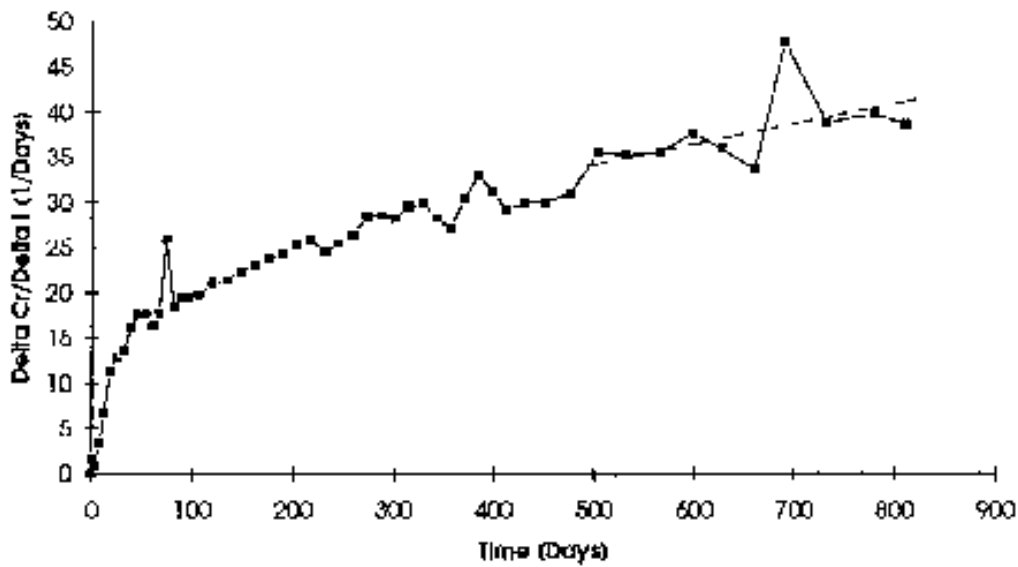


Figure 1 b) Sample C1, 2 cm. The incremental through-diffused amount divided by the time increment,  $^{36}\text{Cl}$ .

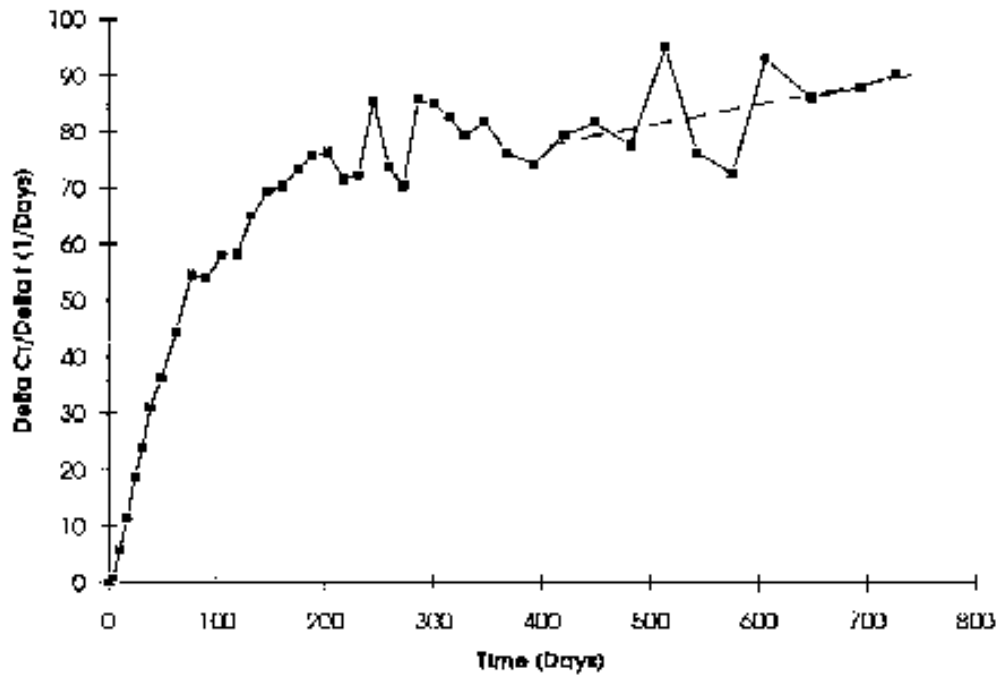


Figure 2 a) Sample C2, 4 cm. The incremental through-diffused amount divided by the time increment,  $^3H$ .

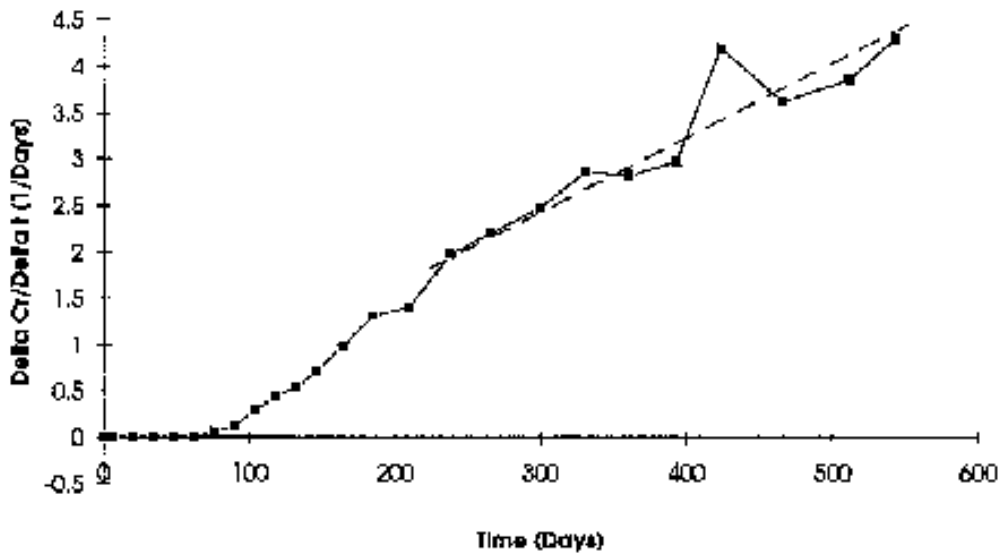


Figure 2 b) Sample C2, 4 cm. The incremental through-diffused amount divided by the time increment,  $^{36}Cl$ .

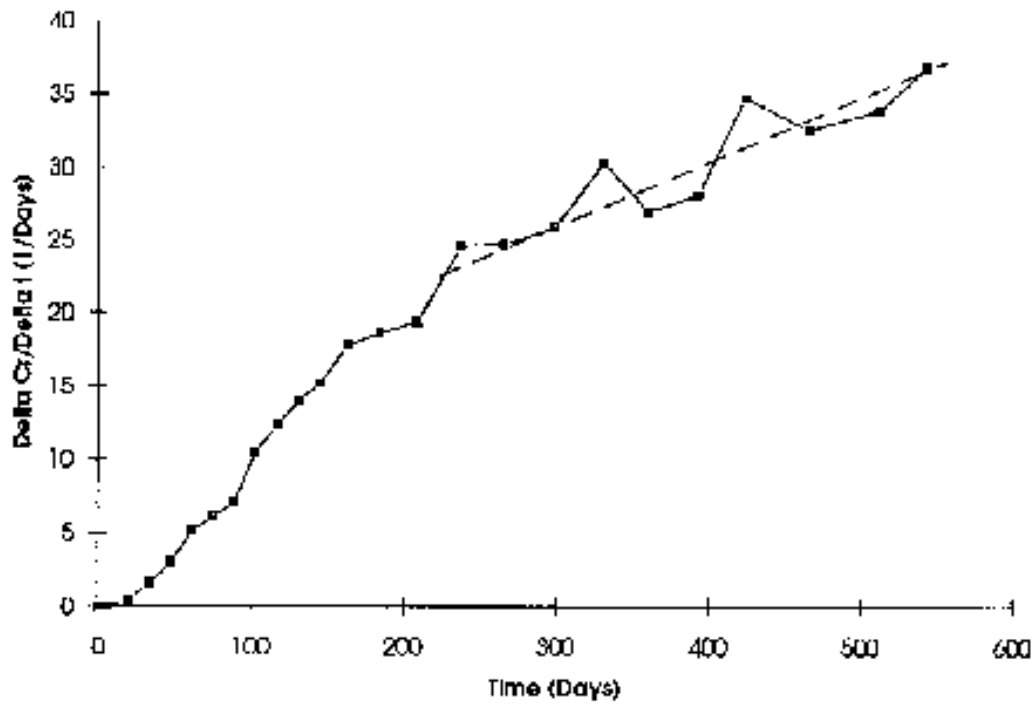


Figure 3 a) Sample C3, 6 cm. The incremental through-diffused amount divided by the time increment,  $^3\text{H}$ .

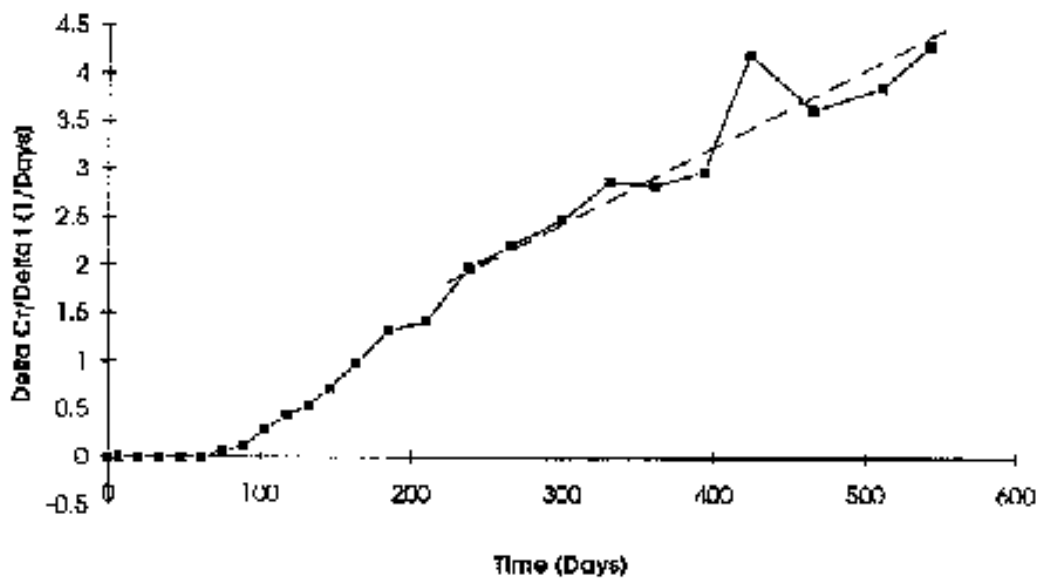


Figure 3 b) Sample C3, 6 cm. The incremental through-diffused amount divided by the time increment,  $^{36}\text{Cl}$ .